


ORIGINAL RESEARCH

Synthesis of silver leaves and their potential application for analysis and degradation of phenolic pollutants

Jianan Sun | Xianhui Gao | Wei Wei 

Department of Basic Medicine, Jinzhou Medical University, Jinzhou, China

CorrespondenceWei Wei, Department of Basic Medicine, Jinzhou Medical University, NO 40 Songpo Road, Linghe District, Jinzhou, China.
Email: weiwei@jzmu.edu.cn**Funding information**

Entrepreneurship Project for College Students of Jinzhou Medical University "Construction of DNA origami sensor and its electrochemiluminescence detection of aflatoxin B1"; National University Student Innovation and Entrepreneurship Training Project, Grant/Award Number: 201910160028

Abstract

A one-pot bottom-up synthesis method was used to synthesise multi-level leaf-like nano-silver (silver leaf) by simply mixing AgNO_3 , L-ascorbic acid, Sodium sodium citrate, and polyvinylpyrrolidone (PVP) in the ethanol-water mixed solvents. Scanning electron microscopy (SEM) characterisations show that the silver leaves have tertiary structures and their sizes are controllable. In addition, silver leaves exhibit excellent Raman enhancement effect (SERS) and chemical catalytic activities for phenolic molecules. Interestingly, the SERS and catalytic activities increase as the size of the silver leaves decrease within a certain range, but when the size is too small, both of these performances weaken. The nanometre size and interstitial structure have a common amplification effect and influence on these activities. The present work not only showed a new method for the synthesis of silver leaves but also could be generalised to find other metallic leaves that could be used as promising heterogeneous catalysts for various reactions. The production of such small-sized silver leaves will facilitate the analysis of phenolic pollutants through Raman enhancement and treat these pollutants through catalytic degradation.

KEYWORDS

catalysis, electrocatalysis, leaf, SERS, silver leaves

1 | INTRODUCTION

Phenolic organic pollutants are common in industrial, agricultural wastes and biological wastewater. The existence of these pollutants has caused great hidden dangers to human health and biosafety. Effectively analysing and removing these pollutants is essential to protect the aqueous environment. Catalytic/electrocatalytic oxidation and reduction are the most effective methods to remove phenolic pollutants. At the same time, sensitive detection of such pollutants has become a prerequisite for the removal of these pollutants. Nanomaterials analysis and treatment of organic pollutants have attracted broad research interest [1]. For example, silver nanomaterials have been investigated in optical detection and pollutant treatment [2]. The pollution treatment efficiency and the sensitivity of the detection are closely related to the structure, size, and shape of the nanomaterials [3]. Until now,

researchers have synthesised various forms of silver and gold nanomaterials, such as cubic [4] and triangular sheet [5], for SERS detection [6], catalysis etc. [4, 7]. Some methods can direct the nanostructure and size, such as template method [8], photochemistry [9] and electrochemistry [10] and other technologies. However, these methods tend to use relatively large amounts of precursors. For example, the template method often brings some foreign products during the synthesis of silver nanomaterials. Although some photochemical and electrochemical methods are relatively simple, the instruments used are relatively expensive, and the energy consumed may cause environmental pollution, which limits the preparation of silver nanomaterials. At the same time, the products may not be well controllable due to the involvement of various conditions [11]. Therefore, it is necessary to further study controllable methods to fabricate silver nanomaterials and have repeatable products.

This is an open access article under the terms of the Creative Commons Attribution-NonCommercial License, which permits use, distribution and reproduction in any medium, provided the original work is properly cited and is not used for commercial purposes.

© 2022 The Authors. *IET Nanobiotechnology* published by John Wiley & Sons Ltd on behalf of The Institution of Engineering and Technology.

The chemical reduction method is normally without requiring complicated conditions. Herein, we use polyvinylpyrrolidone (PVP) and L-ascorbic acid as the capping agent and reducing agent, sodium citrate for shape adjustment, and a one-pot bottom-up synthesis method to obtain silver leaves with controllable sizes for the first time. Although previous studies have reported on silver nanoflowers [12], the size and shape are different, and the degree of controllability is not high. The shapes and sizes of the silver leaves designed in this work can be well controlled. Using the phenolic pollutant rhodamine 6G (R6G) as a typical analyte, it is found that the silver leaves have remarkable SERS effects, which can effectively determine R6G. At the same time, the catalytic activity of this material is significantly higher than that of ordinary silver nanoparticles by the reduction of 4-nitrophenol (4-NP). In the presence of only reducing agents (sodium borohydride, NaBH_4), 4-NP cannot be fastly reduced to 4-nitroaniline (4-AP) in the presence of sphere shape silver nanoparticles (AgNPs). On the other hand, when silver leaves were added, 4-NP was effectively reduced to 4-AP. We also found both the catalytic activities and the SERS performance are depending on the structure of silver nanomaterials. Especially, the catalytic activity shows significant differences when the structure changes, though the silver nanomaterials have similar surface ligands and valence states. This study presents a simple new way to use silver leaves as catalysts to detect and remove phenolic pollutants from wastewater.

2 | RESULTS AND DISCUSSION

In the presence of polyvinylpyrrolidone (PVP), L-ascorbic acid (L-AA) can reduce Ag^+ through the following reactions:

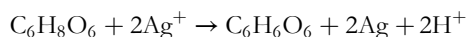


Figure 1 shows the UV-vis spectra of the silver leaves. A strong light absorption peak is located at about 295 nm. This reveals that the silver leaves are covered by the oxidation state of L-AA. On the other hand, because the material has a 3D structure and the overall size is relatively large, almost no

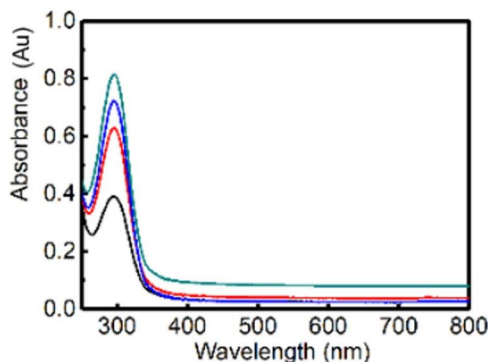


FIGURE 1 The UV-vis spectrum of silver leaves (Leaf1 (green line), Leaf2 (blue line), Leaf3 (red line), and Leaf4 (black line) in size from small to large) (the left figure); SEM image of the silver nanoparticles (AgNPs) for comparison

absorption peak of the sample is observed in the visible light region.

First, AgNPs were prepared (Figure 1, right) as a control for comparison, which was spherical, solid, and had no hierarchical structure. Figure 2 shows the SEM images of silver leaves of different sizes. All silver leaves have a tertiary structure, and each level has a different substructure. It can be seen that the silver leaves are uniformly dispersed. It is worth noting that the size of the particles is very sensitive to the concentration of AgNO_3 . The size of the sample size increases with the increase of the silver concentration (Leaf2>Leaf3>Leaf4). On the other hand, it can be seen that the petals of Leaf4 are compact and have poor looseness compared with other samples (Leaf2 and Leaf3). The internal petals of Leaf2, Leaf3, and Leaf4 are all flaky structures. Only Leaf1 was synthesised without sodium citrate, which showed a thick dendritic internal structure. It can be seen that the concentration of AgNO_3 can guide the size of silver leaves, and sodium citrate can adjust the thickness of the inner petals. Only in the presence of sodium citrate, the petals will become plate-like structures.

Rhodamine 6G (R6G) (10^{-4} M) was selected as a typical target probe. The performance of the above-mentioned four silver leaves for SERS was evaluated (Figure 3). Figure 3a

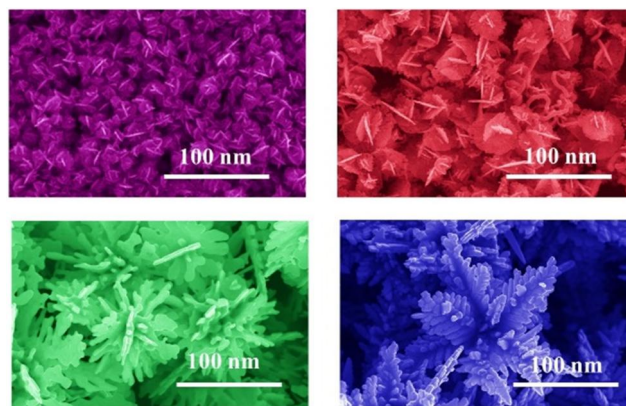
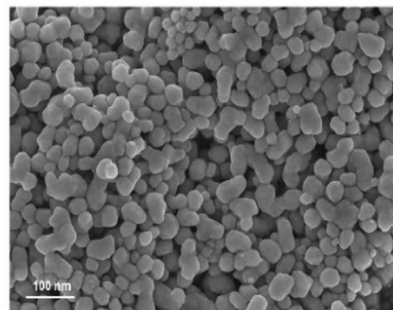


FIGURE 2 SEM images of Leaf4 (top left), Leaf3 (top right), Leaf2 (bottom left), Leaf1 (bottom right). It should be noted only Leaf 1 is synthesised without citrate



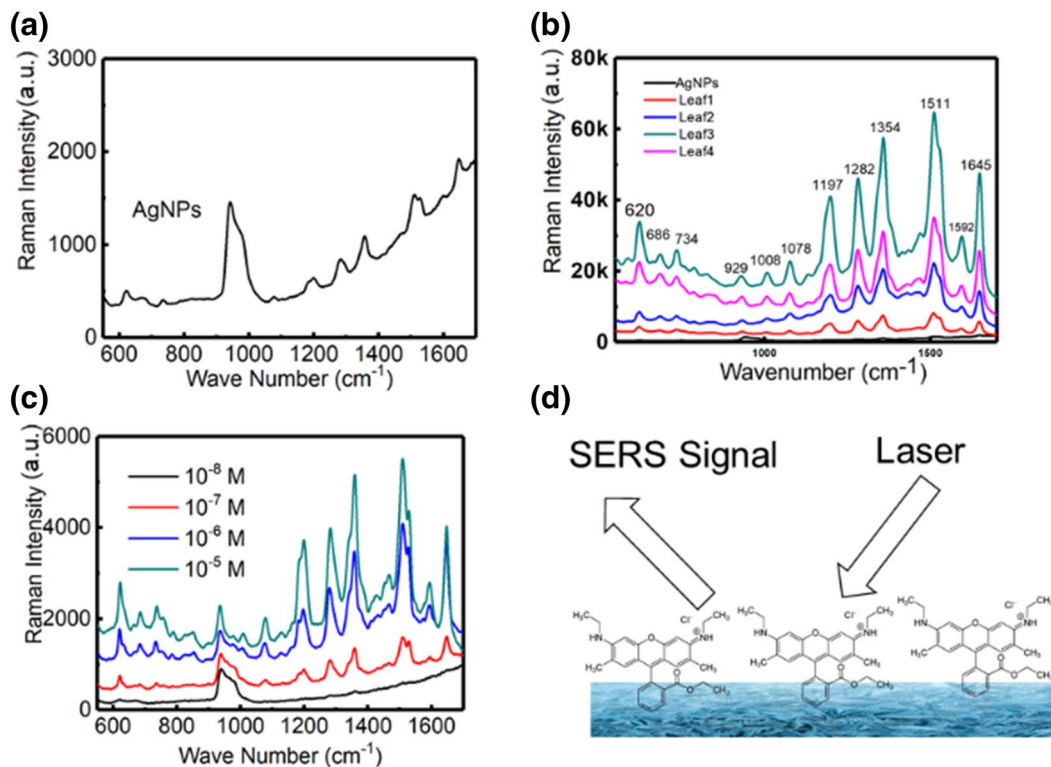


FIGURE 3 (a) Raman spectrum obtained on the surface of spherical silver nanoparticles (AgNPs) on a silicon wafer when 10^{-4} M R6G is in ethanol solution. (b) Raman spectra of R6G on silicon wafers coated with different silver nano-leaves. (c) Raman spectra of different concentrations of R6G on leaf3. (d) A mechanism scheme for the detection of R6G by silver leaf-assisted SERS. It should be noted the Raman intensity for Y-Axis is relative intensity for comparison of different materials

depicts the Raman spectra of the SERS effect of AgNPs, and a relatively weak Raman signal of R6G is observed. Although spherical AgNPs can also have been used for SERS in some references, an aggregate form is required. This means significant SERS enhancement is obtained when an accelerator such as KCl is used to make the nanoparticles tightly arranged on the surface of the silicon wafer [13]. Under non-aggregation conditions, the spherical AgNPs may be randomly scattered, so that the silicon wafer is partially exposed. When R6G is attached to a silicon wafer coated with spherical AgNPs, the molecules cannot be evenly distributed. Therefore, it is difficult to find the accumulation point where Raman is significantly enhanced. On the other hand, the silver leaf is closely connected. For the surface of the silicon wafer coated with silver leaves, several strong peaks can be seen. The peaks at 1645 cm^{-1} , 1592 cm^{-1} , 1511 cm^{-1} , and 1354 cm^{-1} are C-C tensile vibrations. The band at 1197 cm^{-1} is an aromatic C-H bond. The Raman signal intensity of R6G obtained on the surface of the smaller-size silver leaf (Leaf3) is higher than the Raman intensity on the surface of the larger-size Leaf1 and Leaf2 samples. It can be seen that compared with Leaf1 at 1645 cm^{-1} , Leaf3 has a considerable impact on SERS, with an increase of more than three times. Leaf4 is smaller in size, but its Raman signal is relatively weak compared to Leaf3. This may be due to the dense petal structure or even the approximate spherical surface. Therefore, SERS is not only sensitive to the size of nanomaterials, but the structural gap is also crucial. When more molecules are adsorbed to the multi-level and

multi-interstitial surface, it is more conducive to the SERS effect. Then, different concentrations (10^{-5} M, 10^{-6} M, 10^{-7} M, and 10^{-8} M) of R6G solutions were used to study the SERS effect of Leaf3 deposited on the silicon wafer substrate, as shown in Figure 3. At 10^{-8} M, the number of probe molecules adsorbed on the substrate decreases, resulting in low Raman signal intensity. However, when the concentration of R6G increases, the Raman signal is significantly enhanced. This indicates that the SERS phenomenon varies with the concentration of organic dyes and can be applied to its detection.

Since the silver leaves have the potential to detect phenol pollutants in some way, it is also worth wondering whether they can be used to detect the phenol pollutants. Next, we studied the degradation of 4-nitrophenol (4-NP) by NaBH_4 in an aqueous solution. The 4-NP reduction reaction can be selected as a model reaction for evaluating the catalytic activity of various nanomaterials [14]. When 4-NP was combined with NaBH_4 , the colour of the solution was yellow; a maximum absorbance peak at 380–430 nm could be observed due to the presence of 4-NP anions, which might be red or blue shift; hence, the concentration of 4-NP is higher or lower. Herein, the UV-vis of a mixture of 4-NP and NaBH_4 has a maximum absorption at 381 nm. If no catalyst or only AgNPs is added, the reduction will not proceed fastly, the maximum absorption peak change is not obvious with a certain time, and the mixture will remain yellow. This means that there was no significant catalytic activity for the sphere shape AgNPs. Figure 4 shows the UV-vis spectrum of 4-NP in the presence of Leaf3 and

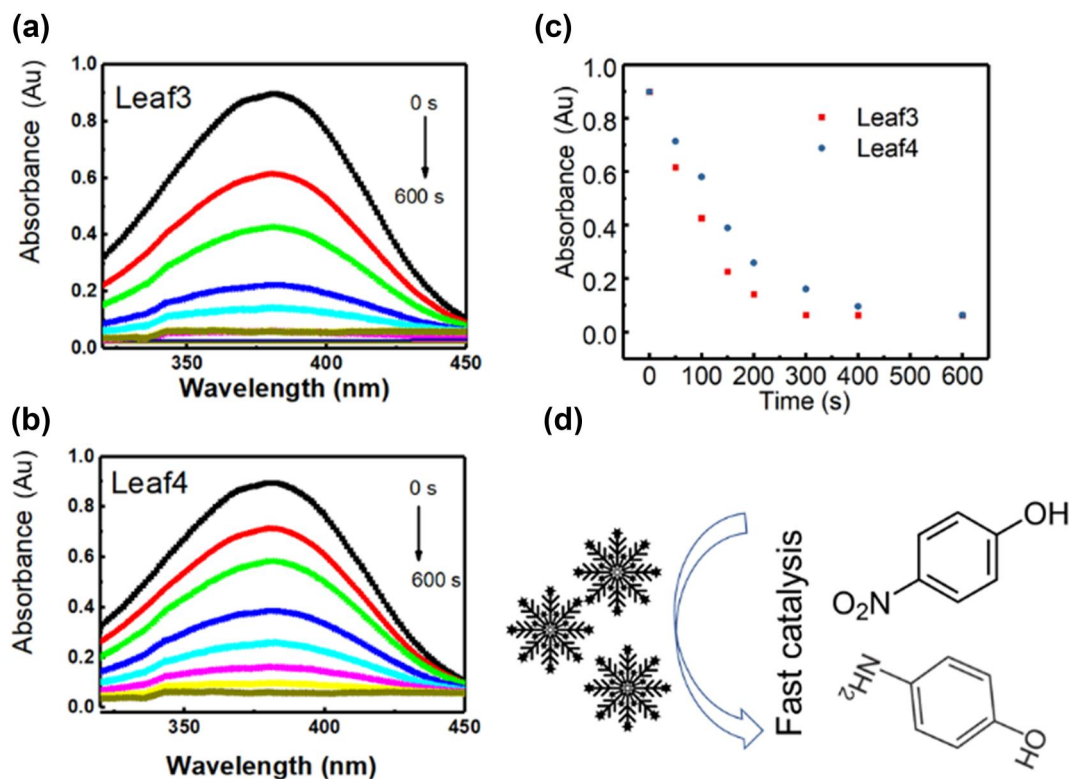


FIGURE 4 The UV-vis spectra of 4-NP were reduced by NaBH_4 as 4-AP in the presence of Leaf3 (a) and Leaf4 (b); the comparison of absorbance changes using Leaf3 and Leaf4 as catalysts (c), and the proposed mechanism (d)

Leaf4. Figure 4b shows that the absorption peak at 381 nm continuously decreases with time and finally disappears within 600 s. The disappearance of the peak represents that 4-NP was converted to the reducing species. When Leaf3 is present, the absorption peak of the sample decreases faster, which indicates that both Leaf3 and Leaf4 have catalytic activity for NaBH_4 reduction of 4-NP, but Leaf3 has higher catalytic activity.

The UV-vis spectra for AgNPs in the presence of 4-NP and NaBH_4 were shown in Figure 5. The absorbance changes insignificantly as a function of time (Figure 5a,b). This further confirms that the ternary structure of silver leaves plays an important role in catalytic activities. Since Leaf3 shows the highest catalytic activities compared to other silver nanomaterials, the reusability of Leaf 3 is investigated (Figure 5c,d). Initially, a random 4-NP solution was reduced by NaBH_4 . Because a relatively high concentration might be present, the peak red shift to 420 nm, but this peak decreases as a function of time once Leaf3 was added (Figure 5c). Instead, another peak at about 310 nm increases, indicating the formation of 4-AP [15]. After the peak completely disappeared, 4-NP was also completely reduced. Furthermore, the solution was used another time and more amounts of 4-NP and NaBH_4 were added. Based on the end of the initial catalytic reaction, the peak at 420 nm continues to decrease, while the absorption peak at 310 nm continues to grow (Figure 5d), indicating more of 4-AP was formed by the reduction of 4-AP. This reaction can repeatedly happen without adding additional catalysts, which indicate Leaf3 can be reused even though they have already been used as a catalyst.

This rapid catalytic degradation of 4-NP provided by this research uses silver leaves as a catalyst to achieve the rapid degradation of toxic 4-NP as less toxic 4-AP. These silver leaves can be loaded on the filter membrane for easy recycling, to avoid external pollution to the environment. Compared with the nanomaterials that have been used in 4-NP degradation (Table 1), the catalytic degradation efficiency of silver leaves is not the highest. However, it is completed by the one-pot method, does not require complicated facilities, is convenient to produce, and has convenient and feasible practical application value. At the same time, insignificant ion release was found when the silver leaves were cultured in water, indicating the raw materials used have the characteristics of low toxicity and do not cause secondary pollution to the aqueous environment.

X-ray diffraction pattern was used to understand the sample we used for the catalytic study (Figure 6a). 100 μL of 25 ppm Leaf3, Leaf4, and AgNPs were dropped on a sliding glass and dried. The peak (2 θ) at about 38° and 44° corresponds to the (111) plane and 220 faces, indicating that the leaves are predominantly composed of Ag single crystals. However, since small amounts of the catalysts were used, the peaks were not remarkable. On the other hand, X-ray photoelectron spectroscopy (XPS) is very sensitive to detecting trace amounts of samples. Thus, XPS is investigated to make a clear understanding of the composition of the silver nanomaterials (Figure 6b–f). The atoms of C, N, O from the surface ligand (PVP), and Ag were found in all three samples, indicating the successful formation of silver nanomaterials. No significant

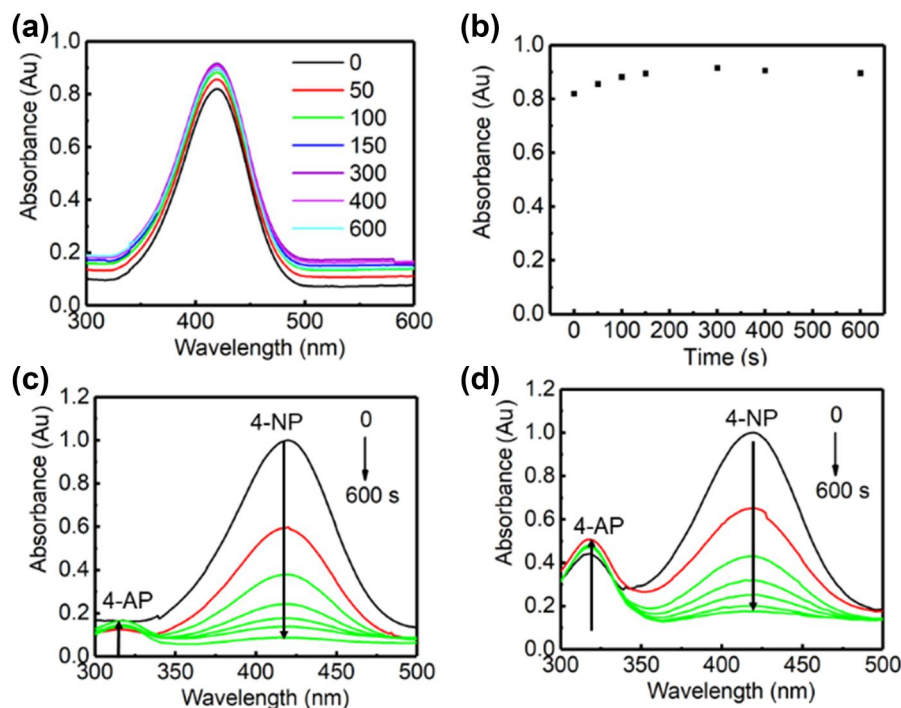


FIGURE 5 UV-vis spectra (a) and absorbance change as a function of time (b) of 4-NP in the presence of NaBH₄ and AgNPs; the UV-vis spectra of 4-NP were reduced by NaBH₄ as 4-AP in the presence of Leaf3 for the use of the first time (c) and the third time (d)

TABLE 1 Nanomaterials used in the catalytic reduction of pollutant 4-NP

Catalyst	Materials	Reaction conditions	Time	Pollutant amounts	Ref.
Fe ₃ C/Au@NG	Ferric chloride, glucose, urea, chloroauric acid, sodium citrate, and nitrogen	Multiple steps; >24h; 800°C	90 s	Large	[16]
CoMn ₂ O ₄ NPs	Tetraethyl silicate, tripolyphosphate, cyclohexane, 1-pentanol, aminopropyltriethoxysilane, cobalt nitrate, manganese nitrate, citric acid etc.	Multiple steps; >48h; 60°C	100 s	Large	[17]
Gold NPs	Chloroauric acid, sodium citrate, PVP, sodium borohydride, and ethanol	Magnetron sputtering (including expensive equipment), 900°C	1000 s	Small	[18]
Silver leaves	Silver nitrate, sodium citrate, PVP, sodium borohydride, and ethanol	One-pot method; <7h; 70°C	500 s	Small	This work

differences were found for the binding energies from C1s, O1s, N1s, and Ag3d, respectively (Figure 6b–f). The narrow width of the Ag3d peaks suggested that only a sharp metallic element silver was present in the Leaf3, Leaf4, and AgNPs, representing the zero valence Ag. The results of XPS indicate that the valence state of all the samples is similar. Thus, the difference of catalytic activities between AgNPs and silver leaves is attributed to the structure difference rather than the composition, surface ligand, or valence difference. The ternary structure of silver leaves facilitates the electron transfer between 4-NP and silver leaf, which was possibly mediated by the gap of the leaf.

3 | CONCLUSION

Through a simple one-pot bottom-up synthesis method, silver leaves of controllable size were obtained. Silver leaves show a stronger SERS effect and catalytic activity than

spherical silver nanoparticles. Among them, Leaf3 has the best performance, which is related to its 3D structure with smaller size and looser multiple gaps compared to other silver leaves. Taking typical phenolic pollutants as an example, this material shows the detection potential of small phenolic pollutants in the field of SERS. At the same time, according to the catalytic principle, silver leaves are likely to play an important role in the degradation of phenolic pollutants in the aqueous environment.

4 | EXPERIMENTAL SECTION

Material: Tannic acid (TA), Ethanol (94.5%), AgNO₃ (99.9%), L-AA (L-ascorbic acid) (99%), NaOH (sodium hydroxide), PVP (MW ≈ 55,000), rhodamine 6G (R6G), NaBH₄ (Sodium borohydride), and 4-nitroaniline (4-NP) were purchased from Sigma-Aldrich. The water used in the experiment was deionised.

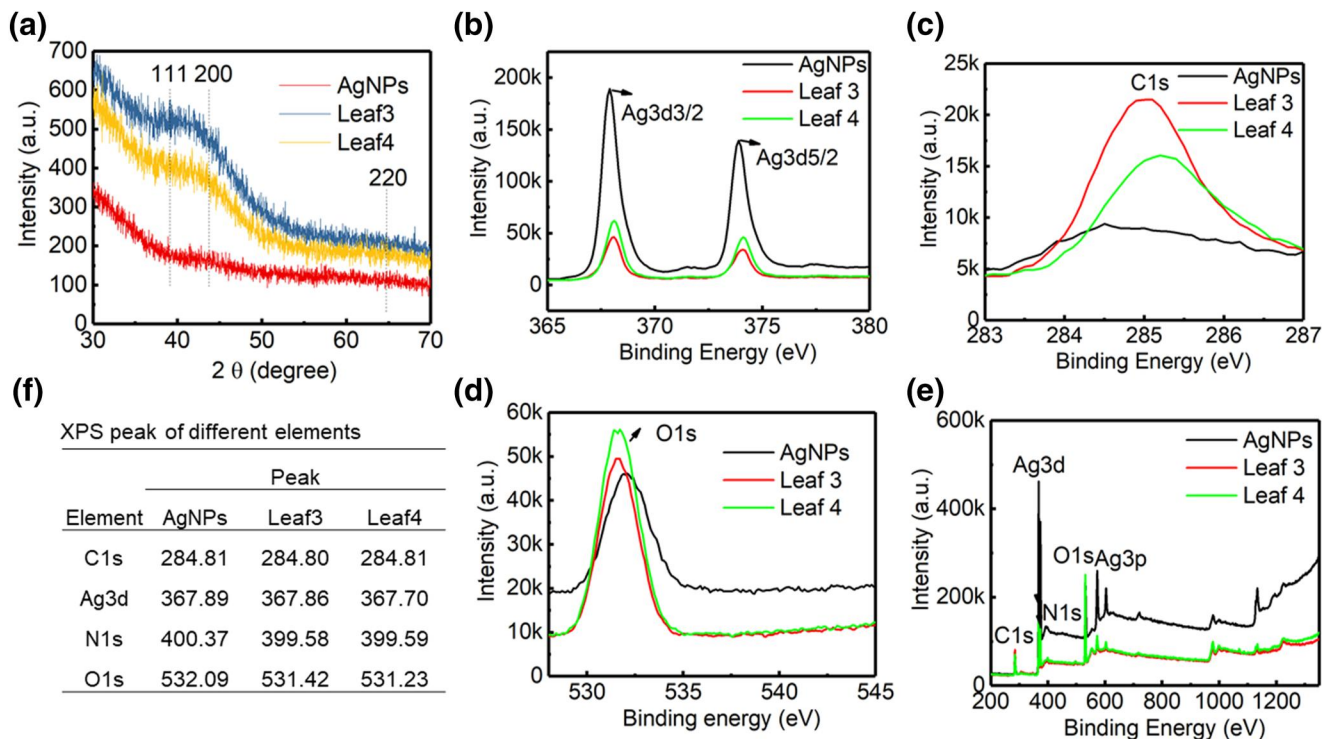


FIGURE 6 X-ray diffraction (a), X-ray photoelectron spectroscopy (XPS) for Ag3d (b), C1s (c), O1s (d), XPS survey (e), and XPS peak table (f) for the narrow scans of different elements for AgNPs, Leaf3, and Leaf4

Synthesis of silver nanomaterials: In a typical one-pot synthesis, different amounts of PVP were dissolved in a vial containing 22 ml of the water-ethanol mixture (V/V = 1:1), and 1.26 ml of 100 mM L-AA was added. Subsequently, 3.0 ml of sodium citrate (10 mM) was combined with the mixture. Next, different volumes of AgNO₃ (10 mM) aqueous solution were added while stirring. The silver leaves named Leaf1–Leaf4 used 500 μ L (Leaf2), 1 ml (Leaf3), 1.5 ml (Leaf4), and 1.5 ml of AgNO₃ following the same procedure. However, no sodium citrate was used for Leaf 1. For comparison, spherical AgNPs were synthesised according to the literature at the same time [5]. A 100 ml aqueous solution containing sodium citrate (5 mM) and tannic acid (TA) was heated in a three-necked round bottom flask with a heating mantle and heated under vigorous stirring for 15 min. A condenser is used to prevent evaporation of the solvent. After the mixture boils, 1 ml AgNO₃ (25 mM) is injected into the solution. The solution immediately turned bright yellow. The size of silver is controlled by adjusting the concentration of TA. By increasing the TA concentration from 0.025 mM to 0.1 mM, 0.25 mM, 1 mM and 5 mM, the size of silver nanoparticles can be adjusted from 10 nm to about 50 nm. We selected nanoparticles with a size close to that of silver leaves for research.

Characterisation and SERS study: After digesting the sample with HNO₃, the original concentration of silver in the prepared sample was determined by Inductively Coupled Plasma Mass Spectroscopy (ICP-MS) (Thermo Scientific). XPS was investigated on an ESCALab 220i-XL electron spectrometer (VG Scientific) using 300 W Al K α radiation. X-ray diffraction

analysis was studied using Ni filtered Cu KR (λ) (1.54 \AA) radiation with X'pert PRO (Pan Analytica) X-ray diffraction unit. For Raman and catalysis studies, the sample is appropriately diluted to 25 ppm. 100 μ L of the sample was dropped on the silicon wafer and dried. SEM confirms the morphology of the silver nanostructures. After that, the sample was immersed in a diluted ethanol solution of R6G for 30 min. The sample was then taken out, rinsed three times with ethanol, and dried in the air. A Renishaw inVia Raman spectrometer coupled with a Leica DMIRB inverted optical microscope was used to obtain SERS from the substrate coated with the research sample. A diode laser was used with an excitation wavelength of 785 nm.

Catalytic research: To study the catalytic activity, 100 μ L of 25 ppm silver leaves were added to 2 ml of 4-nitroaniline (6×10^{-5} M) solution. Then, the freshly prepared NaBH₄ aqueous solution (0.20 ml, 100 mM) was added. The mixture was shaken thoroughly, then transferred to a quartz cuvette with a light path length of 1 cm, and the UV-Vis absorption spectrum (UV-Vis) was recorded to monitor the changes in the reaction mixture. For analysis of the byproduct of silver leaves, the samples were dialysed against a dialysis tube (Thermo Scientific SnakeSkin Dialysis Tubing, 3.5 K MWCO acknowledgements). The released ions outside the tube were analysed by ICP-MS.

ACKNOWLEDGEMENTS

This work is supported by the National University Student Innovation and Entrepreneurship Training Project 201910160028 Preparation technology of ionic liquid drug-

carrying precursors with restricted molecular sieve channels' and Innovation and Entrepreneurship Project for College Students of Jinzhou Medical University 'Construction of DNA origami sensor and its electrochemiluminescence detection of aflatoxin B1'.

CONFLICT OF INTEREST

There is no conflict of interest.

DATA AVAILABILITY STATEMENT

The data will be available under reasonable request.

ORCID

Wei Wei  <https://orcid.org/0000-0002-5486-2111>

REFERENCES

- (a) Naik, S.S., Lee, S.J., Theerthagiri, J., Yu, Y., Choi, M.Y.: Rapid and highly selective electrochemical sensor based on ZnS/Au-decorated f-multi-walled carbon nanotube nanocomposites produced via pulsed laser technique for detection of toxic nitro compounds. *J Hazard Mater.* 418, 126269 (2021); (b) Theerthagiri, J., Lee, S.J., Karuppasamy, K., Arulmani, S., Veeralakshmi, S., Ashokkumar, M., Choi, M.Y.: Application of advanced materials in sonophotocatalytic processes for the remediation of environmental pollutants. *J Hazard Mater.* 412, 125245 (2021); (c) Theerthagiri, J., Lee, S.J., Karuppasamy, K., Park, J., Yu, Y., Kumari, M.L.A., Chandrasekaran, S., Kim, H.S., Choi, M.Y.: Fabrication strategies and surface tuning of hierarchical gold nanostructures for electrochemical detection and removal of toxic pollutants. *J Hazard Mater.* 420, 126648 (2021); (d) Theerthagiri, J., Salla, S., Senthil, R.A., Nithyadharseni, P., Madankumar, A., Arunachalam, P., Maiyalagan, T., Kim, H.S.: A review on ZnO nanostructured materials: energy, environmental and biological applications. *Nanotechnology.* 30, 392001 (2019)
- Supraja, N., et al.: Synthesis, characterization and dose dependent antimicrobial and anticancerous efficacy of phycogenic (*Sargassum muticum*) silver nanoparticles against Breast Cancer Cells (MCF 7) cell line. *Adv. Nano Res.* 6, 183–200 (2018)
- (a) Zhang, L., Lu, H., Chu, J., Ma, J., Fan, Y., Wang, Z., Ni, Y.: Lignin-Directed Control of Silver Nanoparticles with Tunable Size in Porous Lignocellulose Hydrogels and Their Application in Catalytic Reduction. *ACS Sust. Chem. Eng.* 8, 12655–12663 (2020); (b) Huo, D., Kim, M.J., Lyu, Z., Shi, Y., Wiley, B.J., Xia, Y.: One-Dimensional Metal Nanostructures: From Colloidal Syntheses to Applications. *Chem Rev.* 119, 8972–9073 (2019); (c) Lee, S.J., Theerthagiri, J., Choi, M.Y.: Time-resolved dynamics of laser-induced cavitation bubbles during production of Ni nanoparticles via pulsed laser ablation in different solvents and their electrocatalytic activity for determination of toxic nitroaromatics. *Chem. Eng. J.* 427, 130970 (2022)
- Zhu, C., et al.: Detection of dithiocarbamate pesticides with a spongelike surface-enhanced Raman scattering substrate made of reduced graphene oxide-wrapped silver nanocubes. *ACS Appl. Mater. Interf.* 9, 39618–39625 (2017)
- Bhanushali, S., et al.: Photomodulated spatially confined chemical reactivity in a single silver nanoprism. *ACS Nano.* 14, 11100–11109 (2020)
- Lee, S.J., et al.: Nanogap-tailored Au nanoparticles fabricated by pulsed laser ablation for surface-enhanced Raman scattering. *Biosens. Bioelectron.* 197, 113766 (2022)
- (a) Landry, M.J., et al.: Surface-Plasmon-Mediated Hydrogenation of Carbonyls Catalyzed by Silver Nanocubes under Visible Light. *ACS Catal.* 7, 6128–6133 (2017); (b) Bohra, D., et al.: Lateral adsorbate interactions inhibit HCOO⁻ while promoting CO selectivity for CO₂ electrocatalysis on silver. *Angew. Chem. Int. Ed. Engl.* 58, 1345–1349 (2019)
- Han, X., et al.: Template synthesis of NiCo₂S₄/Co₉S₈ hollow spheres for high-performance asymmetric supercapacitors. *Chem. Eng. J.* 368, 513–524 (2019)
- Mostafa, A.M., Menazea, A.A.: Polyvinyl Alcohol/Silver nanoparticles film prepared via pulsed laser ablation: An eco-friendly nano-catalyst for 4-nitrophenol degradation. *J. Mol. Struct.* 1212 (2020)
- Ge, D., et al.: Silver nano-dendrite-plated porous silicon substrates formed by single-step electrochemical synthesis for surface-enhanced Raman scattering. *ACS Appl. Nano Mater.* 3, 3011–3018 (2020)
- Jiang, L., Santiago, I., Foord, J.: High-yield electrochemical synthesis of silver nanoparticles by enzyme-modified boron-doped diamond electrodes. *Langmuir.* 36, 6089–6094 (2020)
- Khan, F.A., et al.: Silver nanoflower decorated graphene oxide sponges for highly sensitive variable stiffness stress sensors. *Small.* 14, e1800549 (2018)
- Langer, J., et al.: Present and future of surface-enhanced Raman scattering. *ACS Nano.* 14, 28–117 (2020)
- Liu, B., et al.: Insight into catalytic mechanisms for the reduction of nitrophenol via heterojunctions of gold nanoclusters on 2D boron nitride nanosheets. *Chem. Nano Mat.* 5, 784–791 (2019)
- Seo, Y.S., et al.: Catalytic reduction of 4-nitrophenol with gold nanoparticles synthesized by caffeic acid. *Nanoscale Res. Lett.* 12, 7 (2017)
- Wang, Y.-L., Dai, Y.-M., Tsai, M.-H.: Highly efficient and recyclable Fe₃C/Au@NG catalyst for 4-nitrophenol reduction. *Catal. Commun.* 149, 106251 (2021)
- Chen, Y., Feng, L., Sadeghzadeh, S.M.: Reduction of 4-nitrophenol and 2-nitroaniline using immobilized CoMn₂O₄ NPs on lignin supported on FPS. *RSC Adv.* 10, 19553–19561 (2020)
- Neal, R.D., et al.: Effect of nanoparticle ligands on 4-nitrophenol reduction: reaction rate, induction time, and ligand desorption. *ACS Catal.* 10, 10040–10050 (2020)

How to cite this article: Sun, J., Gao, X., Wei, W.: Synthesis of silver leaves and their potential application for analysis and degradation of phenolic pollutants. *IET Nanobiotechnol.* 16(3), 78–84 (2022). <https://doi.org/10.1049/nbt.12077>